

Nuclear Charge Radii of ^{229}Th from Isotope and Isomer Shifts

M. S. Safronova,^{1,2} S. G. Porsev,^{1,3} M. G. Kozlov,^{3,4} J. Thielking,⁵ M. V. Okhapkin,⁵
P. Głowacki,^{5,*} D. M. Meier,⁵ and E. Peik⁵

¹*Department of Physics and Astronomy, University of Delaware, Newark, Delaware 19716, USA*

²*Joint Quantum Institute, National Institute of Standards and Technology and the University of Maryland, College Park, Maryland, 20742, USA*

³*Petersburg Nuclear Physics Institute of NRC “Kurchatov Institute”, Gatchina 188300, Russia*

⁴*St. Petersburg Electrotechnical University LETI, St. Petersburg 197376, Russia*

⁵*Physikalisch-Technische Bundesanstalt, 38116 Braunschweig, Germany*



(Received 28 May 2018; published 21 November 2018)

The isotope ^{229}Th is unique in that it possesses an isomeric state of only a few electron volts above the ground state, suitable for nuclear laser excitation. An optical clock based on this transition is expected to be a very sensitive probe for variations of fundamental constants, but the nuclear properties of both states have to be determined precisely to derive the actual sensitivity. We carry out isotope shift calculations in Th^+ and Th^{2+} including the specific mass shift, using a combination of configuration interaction and all-order linearized coupled-cluster methods and estimate the uncertainty of this approach. We perform experimental measurements of the hyperfine structure of Th^{2+} and isotopic shift between $^{229}\text{Th}^{2+}$ and $^{232}\text{Th}^{2+}$ to extract the difference in root-mean-square radii as $\delta\langle r^2 \rangle^{232,229} = 0.299(15) \text{ fm}^2$. Using the recently measured values of the isomer shift of lines of ^{229m}Th , we derive the value for the mean-square radius change between ^{229}Th and its low-lying isomer ^{229m}Th to be $\delta\langle r^2 \rangle^{229m,229} = 0.0105(13) \text{ fm}^2$.

DOI: 10.1103/PhysRevLett.121.213001

The nuclear structure of ^{229}Th is of special interest because of the near degeneracy of its ground state with an isomer whose energy has been evaluated from differences of γ transition energies to be 7.8(5) eV [1]. As a result, ^{229}Th is the only known nucleus with a transition in a laser-accessible region. A possibility to drive this nuclear transition coherently with a narrow-band laser will open a new regime of precision nuclear spectroscopy, with the application to provide the reference for an optical nuclear clock [2]. In addition to the metrology applications, the development of the nuclear clock is of particular interest to searches for physics beyond the standard model of elementary particles due to the potentially very high, $|K| = 10^4$ – 10^5 , sensitivity to the variation of the fine-structure constant α [3]. For comparison, the largest enhancement among the currently operating atomic clocks is $|K| = 6$ [4]. Moreover, the nuclear clock would be sensitive not only to the variation of α , but also to the variation of the ratio of the quark masses m_q to the quantum chromodynamics (QCD) scale Λ_{QCD} [3], which none of the atomic optical clocks are sensitive to. This subject became of even larger interest recently, when the variation of the fundamental constants was directly linked to dark matter searches [5,6]. However, the large enhancement factor K for the nuclear clock remains a subject of open controversy [7,8], which can be resolved via the determination of the Th nuclear parameters [9], including the change in the root-mean-square (rms) charge radius between the isomer

and the Th nuclear ground state, which is the goal of the present work.

General features of the nuclear structure of ^{229}Th are expected to be similar to other nuclei in the actinide region. They are characterized by a combination of collective rotations and vibrations of the quadrupole-octupole deformed core with the single-particle motion of an unpaired neutron [10–12]. The ground state rms charge radii of thorium isotopes from 227 to 230 and 232 have been inferred from measured isotope shifts (IS) of Th^+ [13].

The direct observation of the isomeric ^{229m}Th decay was reported by von der Wense *et al.* [14] and the internal conversion decay half-life of neutral ^{229m}Th was measured by Seiferle *et al.* [15]. Information on the isomer ^{229m}Th became available recently from an experiment with trapped ^{229}Th recoil ions from α decay of ^{233}U [16], indicating a small increase of the rms charge radius of the isomer by about 0.001 fm. Theoretical predictions on this number had been disputed in the context of estimating the sensitivity K of the ^{229}Th nuclear transition frequency to variation of the fine-structure constant. This sensitivity is determined by the change in Coulomb energy ΔE_C between the ground state and the isomer [7–9]. Predictions vary between $\Delta E_C \approx 0$, expected for negligible coupling between the unpaired neutron and the proton core, and a value on the order of 1 MeV, being required as a Coulomb contribution to compensate similar changes of opposite sign in the contributions from the strong interaction in order to arrive at

the small total transition energy of 7.8 eV. Solving this problem based on experimental data on the isomeric charge radius change requires, therefore, a precise determination of the nuclear radii and moments [9].

In order to improve the knowledge on the rms radii difference between isotopes of heavy systems, both reliable *ab initio* calculations and precise isotope shift measurements are required. To achieve the required precision, we have carried out the first calculation of the specific mass shift with a high-precision method that combines configuration interaction (CI) and the all-order linearized coupled-cluster method.

Theoretical calculation.—We carry out isotope shift calculations in Th^+ and Th^{2+} , as well as experimental measurements in Th^{2+} , to extract the difference in the rms radii of the ^{229}Th and ^{232}Th . These calculations are particularly challenging since Th ions are heavy systems with mixed electronic configurations containing $5f$ electrons that are very strongly correlated with core electrons. Therefore, both core-valence and valence-valence correlations have to be accounted for with a high precision. To achieve this, we use the hybrid approach that combines CI and the all-order linearized coupled-cluster methods (CI + all order) [17,18]. The isotope shift separates into the mass shift and the field shift (FS). The mass shift is further separated into the normal mass shift (NMS), simply calculated by the scaling of the experimental transition energy and the specific mass shift (SMS), which is very hard to calculate accurately [19].

The total change in the atomic frequency is given by

$$\Delta\nu^{A'A} = (K_{\text{NMS}} + K_{\text{SMS}}) \left(\frac{1}{A'} - \frac{1}{A} \right) + K'_{\text{FS}} \eta^{A'A}, \quad (1)$$

where $\eta^{A'A}$ can be defined (see, e.g., Ref. [20]) as

$$\eta^{A'A} \equiv \sum_{k \geq 1} c_k \delta \langle r^{2k} \rangle^{A'A} = \delta \langle r^2 \rangle^{A'A} \left(c_1 + \sum_{k \geq 2} c_k \frac{\delta \langle r^{2k} \rangle^{A'A}}{\delta \langle r^2 \rangle^{A'A}} \right). \quad (2)$$

Here,

$$\delta \langle r^{2k} \rangle^{A'A} = \langle r^{2k} \rangle^{A'} - \langle r^{2k} \rangle^A, \quad (3)$$

and c_k are the nuclear parameters.

Assuming that the nucleus can be modeled as a homogeneously charged ball of the radius R , it is easy to show that in the linear approximation over $(\delta R)^{A'A} \equiv R^{A'} - R^A$,

$$\delta \langle r^{2k} \rangle^{A'A} = a_k R^{2k-1} (\delta R)^{A'A}, \quad (4)$$

where a_k are the numerical coefficients and $R \equiv R^{A'} \approx R^A$. As follows from Eq. (4), the ratios $\delta \langle r^{2k} \rangle^{A'A} / \delta \langle r^2 \rangle^{A'A}$ do not depend on $(\delta R)^{A'A}$ in this approximation. Then, introducing the coefficient K_{FS} , defined as

$$K_{\text{FS}} = K'_{\text{FS}} \left(c_1 + \sum_{k=2} c_k \frac{\delta \langle r^{2k} \rangle^{A'A}}{\delta \langle r^2 \rangle^{A'A}} \right), \quad (5)$$

we can rewrite Eq. (1) as follows:

$$\Delta\nu^{A'A} = (K_{\text{NMS}} + K_{\text{SMS}}) \left(\frac{1}{A'} - \frac{1}{A} \right) + K_{\text{FS}} \delta \langle r^2 \rangle^{A'A}. \quad (6)$$

Earlier calculations [13,18] assumed negligible SMS correction for Th; however, we find that it cannot be omitted in a precision calculation. A lowest-order estimate of the SMS correction to the relevant one-electron orbitals in the potential of the Th^{4+} ionic core indicated that SMS can be a few percent of the total IS, requiring further calculations. The NMS correction is only a few megahertz for the transitions of interest to this work and is negligible at the present level of accuracy.

The field shift operator H_{FS} modifies the Coulomb potential inside the nucleus. We use the “finite field” method, which means that perturbation is added to the initial Hamiltonian with the arbitrary coefficient λ : $H \rightarrow H_\lambda = H + \lambda H_{\text{FS}}$. The coefficient λ has to be sufficiently large to make the effect of the field shift significantly larger than the numerical uncertainty of the calculations but small enough to keep the change in the energy linear with λ . We find eigenvalues E by direct diagonalization of H_λ and then find the field shift coefficient K_{FS} as [21,22]

$$K_{\text{FS}} = \frac{5}{6R^2} \frac{\partial E}{\partial \lambda}. \quad (7)$$

It was verified that using the Fermi distribution does not change the results well within the uncertainties of the calculations [23].

The conversion factor from atomic units to SI units for the coefficient K_{FS} is 1 a.u. = 2.3497×10^{-3} GHz/fm². The specific mass shift is calculated by modifying the Hamiltonian with the SMS operator $H \rightarrow H_\lambda = H + \lambda H_{\text{SMS}}$. The SMS coefficient is given by the corresponding derivative $K_{\text{SMS}} = (\partial E / \partial \lambda)$. The conversion factor from atomic units to SI units for the coefficient K_{SMS} is 1 a.u. = 3609.46 GHz/amu.

Experimental method.—In the experiment we use a radio-frequency trap [24] loaded with $\approx 10^6$ Th^+ ions by laser ablation from a target containing ^{229}Th and ^{232}Th and further three-photon ionization of trapped Th^+ to produce $\approx 10^3$ Th^{2+} ions [16]. The ions are cooled close to room temperature by collisions with a high-purity argon buffer gas. The isotopic shift between ^{229}Th and ^{232}Th is measured for three transitions in Th^{2+} from the electronic ground state and the low-lying 63_2 state (levels are labeled by their energy in cm⁻¹ and electronic angular momentum J as subscript, see Fig. 1). We excite the transitions from the state 0_4 to the states 15148_4 and 21784_4 with

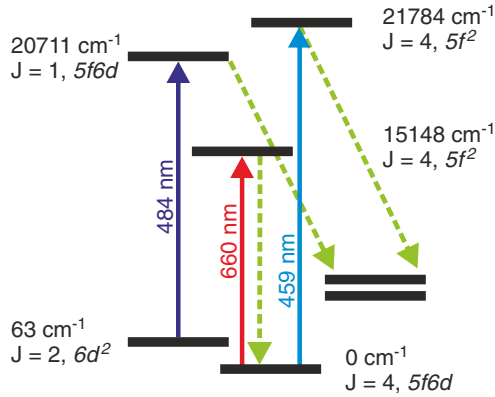


FIG. 1. Partial level scheme of Th^{2+} , showing the transitions relevant to our investigations. The levels are labeled by their energy in cm^{-1} , electronic angular momentum J , and the dominant configuration of the valence electrons. Laser excitation is shown with solid arrows. The detection is provided via fluorescence decay, indicated by dashed lines.

external-cavity diode lasers (ECDLs) at 660 and 459 nm, respectively, and the transition from the level 63_2 to 20711_1 with an ECDL at 484 nm. The 63_2 state is populated by about 30% of the ions in the trap, which provides suitable excitation signals. The output power of all lasers is in the range of 10 mW. We scan the frequency of the ECDLs in the range of ≈ 10 GHz to cover the frequency interval between the ^{232}Th and ^{229}Th isotopes. The laser beams are retroreflected to provide saturated absorption spectroscopy. To measure the frequency detuning of the lasers during the scanning, a temperature stabilized confocal cavity is used. The fluorescence detection is provided by a photomultiplier operating in photon counting mode. For the excitations at 459 and 484 nm, sensitive fluorescence detection of these ions is performed using decay channels at other wavelengths, free from background of laser stray light. The fluorescence signal for the excitation at 660 nm is detected on the same wavelength and therefore is not free from laser background. The three spectra are shown in Fig. 2. The centers of the $^{232}\text{Th}^{2+}$ lines can be easily identified by their nonlinear resonance, but most of the Doppler-free resonances of the $^{229}\text{Th}^{2+}$ hyperfine structure (hfs) are not resolved due to insufficient signal-to-noise ratio, limited by the ion storage time. We therefore identify the center of the hfs for each transition by overlaying the spectroscopy signal with a calculated line shape using the hyperfine constants (A , B) of the involved levels presented in Ref. [25]. The central frequency is then determined for $A = B = 0$. The main contributions to the uncertainties result from the laser frequency interval measurement and from the fit of the calculated hfs to the experimental spectra, giving the same combined rounded value for the uncertainty in all three transitions. While the measured and calculated spectra for the $63_2 \rightarrow 20711_1$ and $0_4 \rightarrow 15148_4$ transitions are in good agreement, we see a mismatch in

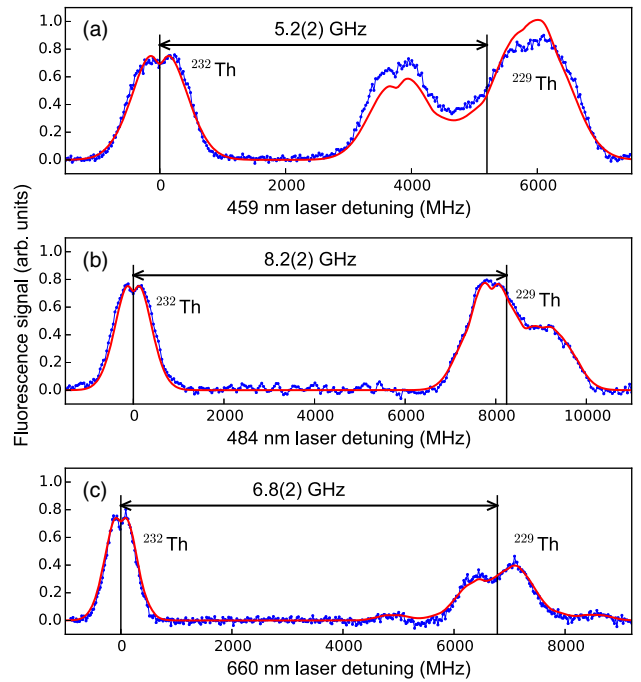


FIG. 2. Fluorescence signals of $^{232}\text{Th}^{2+}$ and $^{229}\text{Th}^{2+}$ obtained with saturated absorption spectroscopy (blue) and calculated line shape (red). The Doppler-free resonances are visible in the $^{232}\text{Th}^{2+}$ resonances, but most of them are not resolved for $^{229}\text{Th}^{2+}$ due to the limited signal-to-noise ratio. The centers of the hyperfine structures of $^{229}\text{Th}^{2+}$ are therefore identified by overlaying the fluorescence signal with the calculated line shape using the hyperfine constants presented in Ref. [25]. (a) Transition $0_4 \rightarrow 21784_4$ at 459 nm, (b) transition $63_2 \rightarrow 20711_1$ at 484 nm, and (c) transition $0_4 \rightarrow 15148_4$ at 660 nm.

amplitudes for the $0_4 \rightarrow 21784_4$ transition, possibly attributed to optical pumping of the decay channels [26]. However, it is still possible to overlap both spectra according to the visible nonlinear resonances and the overall hyperfine splitting (see Supplemental Material for details [27]). The measured isotope shifts are shown in Fig. 2 and listed in Table I. The experimental data for the transition $63_2 \rightarrow 20711_1$ are also presented in Ref. [16], but the fit is reevaluated taking into account saturation effects.

Results.—The results for the FS and SMS $\partial E/\partial \lambda$ derivatives and coefficients are summarized in Table I. We use two different methods for the calculations of the field shift: combination of the CI with many-body perturbation theory (CI+MBPT) [29] and the more accurate CI+all-order method [17]. These approaches allow one to incorporate core excitations in the CI method by constructing an effective Hamiltonian H_{eff} using either second-order MBPT or linearized coupled-cluster methods, respectively. The CI+all-order method includes third- and higher-order corrections to the effective Hamiltonian. Using two methods allows us to establish the effect of the higher orders and to estimate the accuracy of the final results.

TABLE I. Field shift and specific mass shift calculations in Th^+ and Th^{2+} transitions and the extraction of $\delta\langle r^2 \rangle^{232,229}$. Th^+ experimental value is from Ref. [13]. The isotopic shift for the transition $5f6d - 5f^2\ ^3P_0$ is taken from Ref. [16]. Experimental energies from Ref. [28] are given for reference. The differences between the CI + all and CI+MBPT values are given in the column labeled “Diff.”. The experimental IS values are given in column labeled “IS Expt.”.

Ion	Energy Ref. [28]. (cm^{-1})	Electronic configuration	Field shift			Specific mass shift				IS Expt. $\delta\langle r^2 \rangle^{232,229}$	
			$\partial E/\partial\lambda$ CI+MBPT (a.u.)	$\partial E/\partial\lambda$ CI + all (a.u.)	Diff. (%)	K_{FS} CI+all (GHz/ fm^2)	$\partial E/\partial\lambda$ CI+all (a.u.)	K_{SMS} CI + all (GHz/amu)	$\delta\nu_{\text{SMS}}$ CI+all (GHz)	(GHz)	(fm^2)
Th^{2+}	63	$6d^2\ ^3F_2$	-0.000 421	-0.000 372	13%	-36.6	-1.79	-6440	0.364		
	20 711	$5f6d\ ^1P_1$	-0.000 667	-0.000 647	3%	-63.6	-3.30	-11900	0.672		
	29 300	$5f^2\ ^3P_0$	-0.000 805	-0.000 854	6%	-84.1	-4.19	-15100	0.853		
	Transitions	$6d^2 - 5f6d\ ^1P_1$	0.000 247	0.000 274	10%	27.0	1.52	5480	-0.309	8.2(2)	0.315(32)
		$5f6d - 5f^2\ ^3P_0$	0.000 138	0.000 208	34%	20.4	0.88	3180	-0.180	6.2(3)	0.312(42)
Th^{2+}	0	$5f6d\ ^3H_4$	-0.000 713	-0.000 698	2%	-68.7	-3.34	-12 000	0.678		
	15 148	$5f^2\ ^3H_4$		-0.000 910		-89.5	-4.47	-16100	0.909		
	21 784	$5f^2\ ^3F_4$	-0.000 813	-0.000 868	6%	-85.5	-4.31	-15550	0.878		
	Transitions	$5f6d - 5f^2\ ^3H_4$		0.000 212		20.8	1.14	4100	-0.232	6.8(2)	0.338(44)
		$5f6d - 5f^2\ ^3F_4$	0.000 100	0.000 170	41%	16.8	0.97	3510	-0.198	5.2(2)	0.322(53)
Th^+	0	$6d7s^2\ ^2D_{3/2}$	0.000 572	0.000 555	3%	54.6	-2.24	-8090	0.457		
	17 122	$5f6d^2\ J=3/2$	-0.000360	-0.000322	12%	-31.6	-3.69	-13300	0.751		
Transition		$6d7s^2 - 5f6d^2$	0.000 932	0.000 876	6%	86.2	1.45	5240	-0.296	25.01(9)	0.294(17)
Final											0.299(15)

The corresponding results for the derivatives are given in the columns labeled CI + MBPT and CI + all. The difference between these results gives an estimate of the uncertainty of our calculation, listed in the “Diff.” column in percent. For the $5f^2\ ^3H_4$ state, the CI + MBPT approximation gives incorrect level mixing with the $J = 4$ even states leading to a poor result for the IS.

We note that we use a much larger set of the configurations in the CI calculation in comparison with Ref. [18]. The number of configurations was increased to ensure negligible numerical uncertainty in the CI calculation.

The SMS in gigahertz is listed in the $\delta\nu_{\text{SMS}}$ column. The SMS is 3%–4% of the total IS in two Th^{2+} transitions of interest but only 1% for the Th^+ transition listed in Table I. Taking into account that the SMS is small, we calculate it only in the CI+all-order approximation. We roughly estimate its uncertainty as the difference of the one-electron SMS for averaged $6d - 5f$ difference (-0.366 GHz) and final CI+all-order values. Thus, the uncertainties for the $6d^2 - 5f6d$ Th^{2+} and $6d7s^2 - 5f6d^2$ Th^+ transitions are $\sim 20\%$.

The value of $\delta\langle r^2 \rangle^{232,229}$ is extracted by combining experimental and theoretical values according to Eq. (6). The theoretical result for the $6d7s^2 - 5f6d^2$ transition in the Th^+ ion is more accurate, the uncertainty being about 6%, because the FS shifts the levels in opposite directions. As a result, there is no cancellation between upper and lower levels field shifts, leading to higher accuracy in this case. We estimate the uncertainty in the $6d^2\ ^3F_2 - 5f6d\ ^1P_1$ IS in Th^{2+} to be 10% based on the difference

of the CI + MBPT and CI+all-order results. In the other three cases, this procedure is expected to significantly overestimate the uncertainty due to the poor approximation given by the CI + MBPT method. Therefore, we use the absolute uncertainty in the FS constant, 2.7 GHz/ fm^2 , for the $6d^2\ ^3F_2 - 5f6d\ ^1P_1$ transition as the uncertainty for the other three Th^{2+} $6d - 5f$ transitions.

The final value is the weighted average of the two results obtained (i) using the experimental value from this work for the $6d^2 - 5f6d$ transition in Th^{2+} and (ii) using the experimental result [13] for the $6d7s^2 - 5f6d^2$ transition in Th^+ . The weights are calculated as the inverse of the squares of the uncertainties in the $\delta\langle r^2 \rangle^{232,229}$ values. Only the CI+all-order values are used to extract $\delta\langle r^2 \rangle$ while the CI + MBPT results were used for an estimate of uncertainties only. The final uncertainty is dominated by the theoretical uncertainty. The $\delta\langle r^2 \rangle$ values obtained from all other transitions are in agreement with the final result well within the uncertainty.

The final result is $\delta\langle r^2 \rangle^{232,229} = 0.299(15)$ fm^2 . This result is in a good agreement with the present value $0.33(5)$ fm^2 [13] but is 3 times more accurate. A compilation of data on nuclear ground state charge radii [30] gives $\delta\langle r^2 \rangle^{232,229} = 0.334(8)$ fm^2 , relying on Ref. [13] as reference data for thorium, combined with a fit over isotopic sequences of other elements.

We can now give an updated value for the mean-square radius change between ^{229}Th and its low-lying isomer ^{229m}Th , since it is derived from $\delta\langle r^2 \rangle^{232,229}$ and the ratio of the isomeric line shift and the isotopic shift between

^{232}Th and ^{229}Th . Using the ratio of the isomeric and isotopic shifts given in Ref. [16] and our value for $\delta\langle r^2 \rangle^{232,229}$, we obtain $\delta\langle r^2 \rangle^{229m,229} = 0.0105(13) \text{ fm}^2$.

The smallness of the difference of the rms charge radii between isomer and ground state makes it challenging to determine the difference in Coulomb energy as proposed in Ref. [9] because quadrupole and higher-order deformations lead to significant contributions. We have performed numerical calculations of the Coulomb energy in the liquid drop model for shapes in the range of the ^{229}Th ground state deformations $\beta_2 = 0.2$, $\beta_3 = 0.1$, and $\beta_4 = 0.1$ [12,31]. The present uncertainty from the spherical contribution $\delta\langle r^2 \rangle^{229m,229}$ to the Coulomb energy difference is about 30 keV. In order to reach a similar uncertainty for the deformed nucleus (regardless of uncertainty from the nuclear model) the differences in the three parameters β_2 , β_3 , and β_4 will have to be determined experimentally with uncertainties in the low 10^{-3} range. This emphasizes the interest in precision studies of the $^{229}\text{Th}^{3+}$ hyperfine structure, including higher-order contributions beyond the electric quadrupole [32].

We acknowledge financial support from the European Union's Horizon 2020 Research and Innovation Programme under Grant Agreement No. 664732 (nuClock) and from DFG through CRC 1227 (DQ-mat, project B04). This work was supported in part by the Office of Naval Research, U.S., under Grant No. N00014-17-1-2252, and Russian Foundation for Basic Research under Grant No. 17-02-00216.

*Present address: Poznań University of Technology, Poznań, Poland.

- [1] B. R. Beck, C. Wu, P. Beiersdorfer, G. V. Brown, J. A. Becker, K. J. Moody, J. B. Wilhelmy, F. S. Porter, C. A. Kilbourne, and R. L. Kelley, Improved value for the energy splitting of the ground-state doublet in the nucleus ^{229m}Th , Lawrence Livermore National Laboratory Technical Report No. LLNL-PROC-415170, 2009.
- [2] E. Peik and Chr. Tamm, *Europhys. Lett.* **61**, 181 (2003).
- [3] V. V. Flambaum, *Phys. Rev. Lett.* **97**, 092502 (2006).
- [4] N. Huntemann, B. Lipphardt, C. Tamm, V. Gerginov, S. Weyers, and E. Peik, *Phys. Rev. Lett.* **113**, 210802 (2014).
- [5] A. Arvanitaki, J. Huang, and K. Van Tilburg, *Phys. Rev. D* **91**, 015015 (2015).
- [6] A. Derevianko and M. Pospelov, *Nat. Phys.* **10**, 933 (2014).
- [7] A. C. Hayes, J. L. Friar, and P. Möller, *Phys. Rev. C* **78**, 024311 (2008).
- [8] E. Litvinova, H. Feldmeier, J. Dobaczewski, and V. Flambaum, *Phys. Rev. C* **79**, 064303 (2009).
- [9] J. C. Berengut, V. A. Dzuba, V. V. Flambaum, and S. G. Porsev, *Phys. Rev. Lett.* **102**, 210801 (2009).
- [10] N. Minkov and A. Pálffy, *Phys. Rev. Lett.* **118**, 212501 (2017).
- [11] P. V. Bilous, N. Minkov, and A. Pálffy, *Phys. Rev. C* **97**, 044320 (2018).
- [12] P. Butler and W. Nazarewicz, *Rev. Mod. Phys.* **68**, 349 (1996).
- [13] W. Kälber, J. Rink, K. Bökk, W. Faubel, S. Göring, G. Meisel, H. Rebel, and R. C. Thompson, *Z. Phys. A* **334**, 103 (1989).
- [14] L. von der Wense, B. Seiferle, M. Laatiaoui, J. B. Neumayr, H.-J. Maier, H.-F. Wirth, C. Mokry, J. Runke, K. Eberhardt, C. E. Düllmann, N. G. Trautmann, and P. G. Thirolf, *Nature (London)* **533**, 47 (2016).
- [15] B. Seiferle, L. von der Wense, and P. G. Thirolf, *Phys. Rev. Lett.* **118**, 042501 (2017).
- [16] J. Thielking, M. V. Okhaphkin, P. Glowacki, D.-M. Meier, L. von der Wense, B. Seiferle, C. E. Düllmann, P. G. Thirolf, and E. Peik, *Nature (London)* **556**, 321 (2018).
- [17] M. S. Safronova, M. G. Kozlov, W. R. Johnson, and D. Jiang, *Phys. Rev. A* **80**, 012516 (2009).
- [18] M. V. Okhaphkin, D. M. Meier, E. Peik, M. S. Safronova, M. G. Kozlov, and S. G. Porsev, *Phys. Rev. A* **92**, 020503 (2015).
- [19] V. A. Dzuba, W. R. Johnson, and M. S. Safronova, *Phys. Rev. A* **72**, 022503 (2005).
- [20] P. Aufmuth, K. Heilig, and A. Steudel, *At. Data Nucl. Data Tables* **37**, 455 (1987).
- [21] V. A. Korol and M. G. Kozlov, *Phys. Rev. A* **76**, 022103 (2007).
- [22] M. G. Kozlov and V. A. Korol, Notes on volume shift (in Russian), http://www.qchem.pnpi.spb.ru/kozlov/My_papers/notes/notes_on_is.pdf.
- [23] M. R. Kalita, J. A. Behr, A. Gorelov, M. R. Pearson, A. C. DeHart, G. Gwinner, M. J. Kossin, L. A. Orozco, S. Aubin, E. Gomez, M. S. Safronova, V. A. Dzuba, and V. V. Flambaum, *Phys. Rev. A* **97**, 042507 (2018).
- [24] O. A. Herrera-Sancho, M. V. Okhaphkin, K. Zimmermann, Chr. Tamm, E. Peik, A. V. Taichenachev, V. I. Yudin, and P. Glowacki, *Phys. Rev. A* **85**, 033402 (2012).
- [25] R. A. Müller, A. V. Maiorova, S. Fritzsche, A. V. Volotka, R. Beerwerth, P. Glowacki, J. Thielking, D.-M. Meier, M. Okhaphkin, E. Peik, and A. Surzhykov, *Phys. Rev. A* **98**, 020503 (2018).
- [26] I. Sydoryk, N. N. Bezuglov, I. I. Beterov, K. Miculis, E. Saks, A. Janovs, P. Spels, and A. Ekers, *Phys. Rev. A* **77**, 042511 (2008).
- [27] See Supplemental Material at <http://link.aps.org/supplemental/10.1103/PhysRevLett.121.213001> for more details on the determination of the isotopic shift of the transition $0_4 \rightarrow 21784_4$.
- [28] J. Blaise and J.-F. Wyart, Thorium energy levels, <http://web2.lac.u-psud.fr/lac/Database/Tab-energy/Thorium/Th-el-dir.html>.
- [29] V. A. Dzuba, V. V. Flambaum, and M. G. Kozlov, *Phys. Rev. A* **54**, 3948 (1996).
- [30] I. Angeli and K. P. Marinova, *At. Data Nucl. Data Tables* **99**, 69 (2013).
- [31] P. Möller, J. R. Nix, W. D. Myers, and W. J. Swiatecki, *At. Data Nucl. Data Tables* **59**, 185 (1995).
- [32] K. Beloy, *Phys. Rev. Lett.* **112**, 062503 (2014).